*Mon. Not. R. astr. Soc.* (1983) **205**, 1103–1116

# The luminosity of particle beams from thick accretion discs

Ramesh Narayan, Rajaram Nityananda and
Paul J. Wiita★ *Raman Research Institute, Bangalore 560 080, India*

Received 1983 April 10; in original form 1982 November 9

**Summary.** We investigate the interaction of the radiation produced in the funnels of thick, highly luminous accretion discs with the walls of these funnels. Some processes not considered in an earlier discussion have been included. The turbulent mixing of the surface layer with deeper regions acts to reduce the luminosity associated with outflowing matter. The modification of the radiation field by the moving walls is also important. We find, for the specific funnel geometry studied, corresponding to a radiation luminosity of 8.5 times the Eddington limit $L_E$, that up to $1.5\,L_E$ can be carried away as a particle beam, even for an optically thin funnel. This particle luminosity is sensitive to the sound velocity and the mixing efficiency in the walls. The implications for modelling of thick accretion discs are briefly discussed.

## 1 Introduction

Over the past few years a theory of active galactic nuclei involving geometrically thick radiation supported accretion discs around black holes has been developed, both in a general relativistic framework (Lynden-Bell 1978; Jaroszyński, Abramowicz & Paczyński 1980; Sikora 1981, hereafter Sk) and in the Newtonian or pseudo-relativistic approximation (Paczyński & Wiita 1980; Abramowicz, Calvani & Nobili 1980; Sikora & Wilson 1981, hereafter SW). The basic concepts involved in these models include: (a) global balancing of the energy generated by viscosity with that radiated from the disc surface, (b) assumption of a plausible angular momentum distribution and (c) determination of the shape of the disc as an equipotential of gravitational plus centrifugal forces (e.g. Kozlowski, Jaroszyński & Abramowicz 1978). In thin disc theory, it is known that the luminosity approaches the Eddington limit

$$L_E = \frac{4\pi G M_c}{\kappa} \tag{1}$$

as the accretion rate approaches a critical value $\dot{M}_{cr} = 8\pi c r_0/\kappa$ where $M$ is the mass of the accreting body, $\kappa$ is the opacity (usually $0.4\,\mathrm{cm^2\,gm^{-1}}$ as electron scattering dominates in

★ Permanent address: Paul J. Wiita, Department of Astronomy and Astrophysics (E1), University of Pennsylvania, Philadelphia PA 19104, USA.

the case of interest) and $r_0$ is the radius of the inner edge of the disc. As pointed out by Shakura & Sunyaev (1973), when $\dot{M} \gtrsim \dot{M}_{cr}$, the disc must thicken. One possibility is that the flow becomes essentially radial with a wind carrying off the excess material (e.g. Meier 1982a, b, c). However, if the effective viscosity in the bulk of the disc is sufficiently small, it seems that a pair of funnels can form along the angular momentum axis of the accreted material. These funnels have the geometry (Lynden-Bell 1978) and the high luminosity (Paczyński & Wiita 1980) that appear to be necessary for producing collimated jets in quasars and other galactic nuclei (Rees *et al.* 1982 have, however, suggested a different mechanism for non-QSO radio sources). Early estimates of high velocities (Lorentz factor $\gamma \simeq 2$) produced by radiative acceleration of test particles in such funnels (Abramowicz & Piran 1980) have not been borne out by subsequent calculations (Sk; SW; Piran 1982) where values of $\gamma \simeq 1.15$ for ordinary electron proton plasma have been found.

Although thick disc models are constructed to have normal forces at the surface in balance, there are unbalanced tangential forces. These were considered by most authors to be unimportant or to drive slow meridional motions within the disc (Paczyński 1978, private communication; Sk). Recently, however, Nityananda & Narayan (1982, henceforth NN) have shown that these unbalanced forces can be very important for narrow funnels. From geometric considerations, they argued that a funnel of small semi-opening angle $\phi$ (Fig. 1) cannot have luminosity exceeding $\phi^2 L_E$ if it is to be in strict equilibrium. Allowing in a simple way for momentum transfer by flow induced shear stresses, they suggested a luminosity up to $\sim \phi L_E$ was possible. Since the typical luminosity in thick disc models is $\sim L_E/\phi$, they argued that a significant part of the luminosity must be in outflowing matter and that this should be included for consistency.

We can give a rather general argument for the potential importance of particle outflow in narrow funnels. Near the bottom of the funnel, where much of the luminosity is generated, the radiation field has a large isotropic component. Looking at a unit area oriented normal to the axis of the funnel, we therefore have a flux $F_s$ crossing it upwards and an almost equal flux in the opposite direction. The associated momentum flux, i.e. radiation pressure, is given by $4F_s/3c$ in the isotropic case. The vertical momentum crossing a section of radius

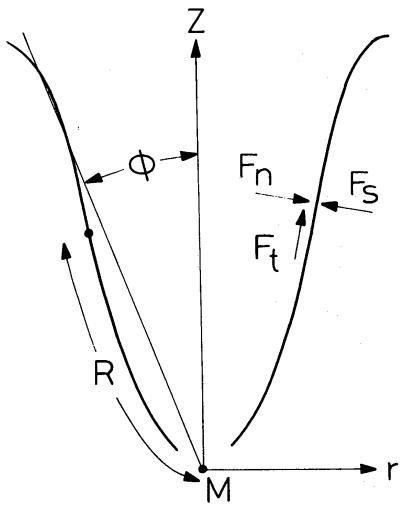


**Figure 1.** Geometry of a funnel of semi-opening angle $\phi$ in a thick accretion disc around a black hole at $M$ (schematic). The cylindrical coordinates are r and z, while R is a coordinate along the funnel surface. The fluxes $F_t$, $F_n$ and $F_s$ along the tangential, inward normal and outward normal are used to characterize the radiation field.

'$r$' is thus $4\pi r^2 F_s/3c$. The crucial point is that $\pi r^2 F_s$ is significantly greater than the net luminosity $L_r$ which finally leaves the funnel, carrying away a momentum $L_r/c$ since it is well collimated. We conclude that a large fraction of the momentum injected by radiation into the lower part of the funnel is not contained in the radiation which finally escapes, and is therefore deposited in the walls. In the extreme case when the walls are accelerated to relativistic speeds, the particle luminosity, $L_p$, is thus of the same order as $L_r$ or greater, while in the opposite case of low particle velocities, the energy associated with this momentum is very small.

Motivated by the 'momentum problem' just described, we have tried to analyse various accelerating and drag forces which act on the funnel walls. In the process, we have re-examined the assumptions and approximations in the earlier work of NN. Since the calculations require knowledge of the radiation field, we have used the results of Sk for a model funnel with a luminosity of $8.5\,L_e$, making some changes to allow for the moving walls. We have not attempted a fully self-consistent determination of the radiation field with moving walls. Our results confirm the general validity of the points made by NN. However, $L_p$ is significantly less than their estimates and depends sensitively on two factors: (i) the sound speed $\beta_s \equiv v_s/c$ in the outer layers of the funnel, (ii) the ratio $\alpha^{1/2}$ of the largest (rms) fluctuating component of the turbulent velocity to the sound speed $v_s$.

The rest of the paper is organized as follows. Section 2 shows that the radiative acceleration of the surface layers of the funnel induces strong Kelvin–Helmholtz instabilities. These mix the surface layer with the interior on a time-scale short compared to that for acceleration, and carry tangential momentum away from the surface. Appendix A discusses a simple mixing length model for the turbulent momentum transport. The velocity of the surface layer can only grow very slowly (i.e. logarithmically) until turbulent velocities become of the order of the sound speed. Thereafter, the drag saturates and the surface layer can accelerate.

In Section 3 we discuss the radiation field in the funnel, drawing on the work of Sk but making some changes to allow for the moving walls in order to conserve the total radiative luminosity. The tangential momentum delivered to the funnel walls is calculated on a simple model. Appendix B shows that the errors involved in this approximation are not large for the kind of radiation field expected in the funnel. We also compute the tangential momentum carried away from a surface element by radiation.

Section 4 combines the results of the two previous sections to set up the momentum balance equation for the surface layer. Numerical results are given for the funnel and radiation field studied by Sk. Section 5 gives our conclusions and a discussion.

## 2 Turbulent mixing and drag

### 2.1 KELVIN–HELMHOLTZ INSTABILITIES

Let us consider a fluid layer of depth $\mathbf{a}$, moving at a velocity $\mathbf{v}$ with respect to an underlying fluid at rest (Fig. 2). We would argue that the rate of growth of perturbations at the interface would only be underestimated if we use results for the standard case of two semi-infinite fluids in relative motion. We use the results of Turland & Scheuer (1977) (see also Blandford & Pringle 1977) which are applicable when the relative velocity and the sound speed can be relativistic. As long as $v < v_s$, some perturbations continue to grow at rates $\sim vk$ ($k$ = wavevector). For $v > v_s$ only perturbations sufficiently oblique to $\mathbf{v}$ will grow, with rates $\sim v_s k$. Although the shortest wavelength modes grow most rapidly, those with wavelengths $\sim \mathbf{a}$ are most relevant for mixing the layer with the substrate. Allowing for the

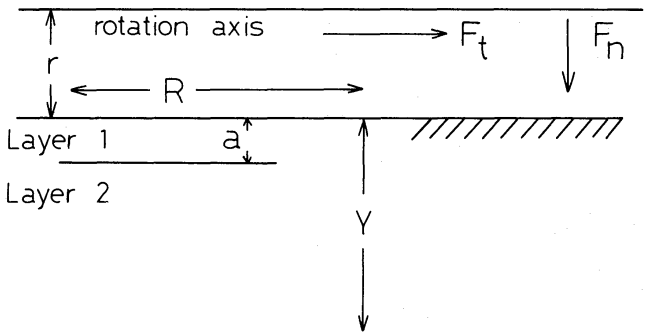


**Figure 2.** Momentum transfer from the surface layer (labelled 1) to the bulk is idealized by considering a constant shear $\sigma$ acting on the inner wall of a cylinder for $R > 0$. The velocity field $U(R, y)$ is calculated in Appendix A. The effective depth of the layer over which the tangential flux $F_t$ acts is denoted by **a**.

retardation in growth rates due to the mildly relativistic sound speed (at most a factor of 2.5 – Turland & Scheuer 1977), we have growth time-scales $t_g$ given by

$$t_g \lesssim \max(a/v, a/v_s). \tag{2}$$

We assume that a time $\sim 5t_g$ is needed for significant sharing of mass and momentum between adjacent layers. This is to be compared to the time-scale $t_a$ for acceleration of the surface layer over the characteristic length scale $R$ of the funnel (Fig. 1). Typically, $t_a = 2R/v$. We thus find that

$$t_a/t_{mix} \sim \frac{2R}{5a}\ (v < v_s) \qquad \text{or} \qquad \frac{2Rv_s}{5av} \qquad \text{for} \qquad v > v_s. \tag{3}$$

The depth **a** is discussed in detail in the next section and in Appendix B but corresponds to an optical depth $\sim 1$, i.e. $a \sim 1/\kappa\rho_0$. Using typical $\rho_0$ values from Wiita (1982), we find that typically $R/a \sim 10^4$ and invariably $R/a > 50$. It is thus clear that the mixing is extremely effective and we can model it as fully developed turbulence. Analogous results were found by Elmegreen (1979) who studied the interaction of a protostellar wind with the surrounding preplanetary nebula.

The standard analysis predicts that the interface between the moving layer and vacuum is strictly stable (Blandford & Pringle 1977). However, convective motions, flows along magnetic field lines and the powerful subsurface mixing just discussed should all lead to a 'wind'. Such a wind has in fact been invoked (e.g. Sk) to feed the funnel with 'test particles' that can be accelerated and collimated into beams. In the rest of this paper we shall ignore this factor but assume that the funnel still remains optically thin, so that we can use the radiation field computed for vacuum funnels. Optically thick funnels would of course require an entirely different approach (Abramowicz, Calvani & Nobili 1983).

## 2.2 TURBULENT DRAG FORCES

Because of the strong mixing, we ignore microscopic and radiative viscosity* and use results from turbulent shear flows (Monin & Yaglom 1971). If $\sigma$ is the applied shear and $\rho_0$ the density, the characteristic velocity $v_* = (\sigma/\rho_0)^{1/2}$ is a measure of the random velocities in the

* Radiative momentum transfer can become comparable to that arising from mixing when there is a steep velocity gradient near the surface (see equation 15 and the discussion in Section 5).

turbulent flow. Defining the $R$ and $Y$ directions along and perpendicular to the layer (Fig. 2), the fluctuating velocity components $U_R$ and $U_Y$ satisfy

$$\overline{U_R U_Y} = v_*^2; \qquad \overline{U_R U_R} \simeq (2.2 v_*)^2; \qquad \overline{U_Y U_Y} \simeq v_*^2. \tag{4}$$

The first equality follows from the definition of shear stress while the second and third are experimental results.

We now make the assumption that the rms value of $U_R$, the largest turbulent velocity component, cannot exceed a multiple $\alpha^{1/2}$ of the sound speed, where the factor $\alpha$ should be of order 1 but is retained explicitly to reflect the uncertainty in this estimate. The maximum stress which can be transmitted is thus given by

$$\sigma_{max}/\rho_0 = v_{*,max}^2 = \frac{(\overline{U_R U_R})_{max}}{4.84} = \alpha v_s^2/4.84. \tag{5}$$

We note that a similar estimate for the maximum stress has been given by Shakura & Sunyaev (1973) in the context of thin, Keplerian accretion discs. We also note that this criterion should be applied in a frame moving with the mean velocity.

We thus arrive at the following physical picture. The flux of radiation $F_t$ parallel to the funnel walls (Fig. 1) deposits tangential momentum at a rate $\sigma$ into the surface layer of thickness **a**. So long as $\sigma$ does not exceed the critical value (5) there is efficient mixing and the velocity of the surface layer grows very slowly (equation A12, Appendix A). For an applied stress greater than $\sigma_{max}$, we have acceleration of the surface layer with a drag given by (5) coming from the layers below. In what follows we use the subscripts 1 and 2 to refer to the surface layer and the one below (Fig. 2). From (A15, Appendix A), the maximum stress which the 2 layer can carry is given in the rest (funnel) frame by

$$\sigma_{max}^{RY} = \frac{\alpha \rho_0 v_s^2}{4.84} \gamma_2 (1 + \beta_2 \beta_{12}). \tag{6}$$

where $c\beta_2$ = velocity of layer 2, $\gamma_2 = (1-\beta_2^2)^{-1/2}$ is the corresponding Lorentz factor, $\beta_{12}$ the velocity of the layer 1 relative to 2, and $\rho_0$ the proper rest mass density of either layer.

## 3 Radiation field and tangential stresses

### 3.1 RADIATION FIELD IN THE FUNNEL

The outgoing radiation at any point on the funnel surface is described by giving $F_s$, the self-flux. The incoming radiation field has a significant angular dependence, and two important quantities derived from it are the normal flux $F_n$ and the tangential flux $F_t$. Fig. 1 shows these fluxes schematically. For steep funnels, with a small semi-angle $\phi$, the net outgoing flux $(F_s - F_n)$ is a much smaller quantity than either $F_s$ or $F_n$, over much of the funnel, because of the strong 'reflection effect'. This net flux is what enters the normal equilibrium condition at the surface and is determined by the funnel geometry and angular momentum distribution (Sk; SW). In the following, we denote the radiation fluxes computed by Sikora (1981) by the subscript 'Sk'. Our calculations of particle luminosity are basically for his funnel model, with some modifications of the radiation field to allow for the motion of the walls, conserving the total radiation luminosity $L_r$. Since the tangential flux $F_t$ integrated over the funnel cross-section at any point gives $L_r$ below that level, we have retained the $F_t$ values computed by Sk. However, the fluxes $F_s$ and $F_n$, which are determined from the equilibrium condition and the reflection effect, will now be different

when we allow for the motion of the funnel walls. Rather than solve this problem *ab initio*, we have modified the self-flux computed by Sikora to ensure that the *escaping* luminosity remains the same. Thus, if $F_{s1}$ is the self-flux emitted isotropically from layer 1 in its rest frame, the specific intensity* in the direction of motion in the funnel frame is enhanced by a factor $(1+\beta_1)^2/(1-\beta_1)^2$. It can be checked for $\beta_1 < 0.5$ and $\phi \sim 10^\circ$ that this enhancement holds for all rays which escape and not just in the forward direction. To obtain the same escaping luminosity with moving walls, we thus write

$$F_{s,\,Sk} = F_{s1}\left(\frac{1+\beta_1}{1-\beta_1}\right)^2. \tag{7}$$

### 3.2 PENETRATION OF RADIATION AND TANGENTIAL STRESSES

We first discuss the incoming radiation at the funnel surface (subscript 'in'). The tangential (R-component of) momentum crossing a unit area of the funnel wall (i.e. in the $Y$ direction of Fig. 2) is denoted by $T^{RY}$. In terms of a unit vector $\mathbf{n}$ and the specific intensity $I$, we can write

$$cT^{RY}_{in} = \int I_{in}(\mathbf{n}) n_R n_Y \, d\Omega. \tag{8}$$

In the same notation, the tangential flux $F_t$ is given by

$$F_{t,\,in} \equiv T^{0R}_{in} = \int I_{in}(\mathbf{n}) n_R \, d\Omega. \tag{9}$$

If the effective depth of penetration of $F_t$ is $a$, we can write the tangential force on a unit area as $F_t(\kappa/c)\rho_0 a$. For consistency, this equals the tangential momentum entering viz., $T^{RY}_{in}$. The optical depth $\kappa\rho_0 a$ over which the penetration is effective in thus the ratio $cT^{RY}_{in}/T^{0R}_{in}$. Of course this will depend on the precise angular dependence of the radiation field. For a field with the simplest kind of anisotropy, viz. $I(\mathbf{n}) = I_0 + I_1 n_R$, we have $cT^{RY}_{in} = (\pi/4)I_1$, $T^{0R}_{in} = (2\pi/3)I_1$. The effective optical depth for penetration is thus 3/8. Appendix B considers a more general radiation field which perhaps mimics that in a funnel more closely. The penetration optical depth does not vary too much over the range of interest, and we thus adopt

$$cT^{RY}_{in} = \frac{3}{8} F_{t,\,in}; \qquad a = 3/(8\kappa\rho_0). \tag{10}$$

We also need the tangential momentum carried away by the outgoing flux. This quantity is zero in the frame 1, in which there is a flux $T^{0Y}_1 = F_{s1}$ in the $Y$ direction. A Lorentz transformation gives

$$cT^{RY}_{out} = \gamma_1\beta_1 F_{s1}. \tag{11}$$

Further, the contribution of $F_{s1}$ to the tangential flux in the funnel frame is also given by a transformation

$$T^{0R}_{out} = \frac{8}{3}\gamma_1^2\beta_1 F_{s1}. \tag{12}$$

*We use the specific intensity integrated over frequency, which behaves as (frequency)$^4$ under Lorentz transformations.

From the requirement of fixed total luminosity we have

$$F_{t,\,Sk} = T_{in}^{0R} + T_{out}^{0R}. \tag{13}$$

Strictly speaking, this condition applies only to the integral over the funnel cross-section, but for steep funnels the variation of the fluxes over the cross-section is not strong. Equations (7) and (10–13) give us all the quantities entering the momentum balance for the surface layer, which we discuss in the next section.

## 4 Momentum balance and equations of motion for the surface layer

As a preliminary step, we need to discuss the sound speed. This is given in terms of the radiation energy density $E$ by

$$v_s^2 = \frac{4p_{rad}}{3\rho_0} = \frac{4E}{9\rho_0} = \frac{16F_s}{9\rho_0 c}. \tag{14}$$

Here we have expressed the self-flux $F_s$ in terms of $E$ through $F_s = cE/4$ which is strictly true only for an isotropic radiation field but is quite accurate in the disc interior. While Wiita (1982) has given estimates of $p_0(R)$ and $\rho_0(R)$ for a range of model funnels, his calculations do not include the reflection effect which tends to enhance $F_s$ by a factor ranging from 10 to $10^4$ (SW). However, the reflection effect also enhances $\rho_0$. Bearing these factors in mind, we investigate the cases $\beta_s = 0.01$, 0.03 and 0.1, and treat $\beta_s$ as a constant over the funnel. (The results of Wiita 1982 show a variation of only a factor of $\sim 2$). The dissipation associated with the mixing will heat the material and we assume that this is allowed for in choosing $\beta_s$.

Another point concerns the relationship between $F_{s2}$, the isotropic self-flux crossing from layer 2 to layer 1 (viewed in the 2 frame) and $F_{s1}$, the flux directed from layer 1 (assumed to be optically thick) either into the funnel or into layer 2. Viewed in the funnel frame, we assume that the net energy transfer is zero, because $F_s - F_n \ll F_s, F_n$. This leads to

$$\gamma_1 F_{s1} = \gamma_2 F_{s2}. \tag{15}$$

Since the Lorentz factors are quite close to 1 and $F_{s2}$ is needed basically for the sound speed determination, this approximation should be adequate.

Consider now the element of the surface layer shown in Fig. 3, of thickness **a**, radius **r**, and slant length $\Delta R$. The tangential momentum entering a unit area of its inner surface per unit time is given by $T_{in}^{RY} = (3/8)F_{t,\,in}/c$ (equation 10). Then we have a stress $T_{out}^{RY}$

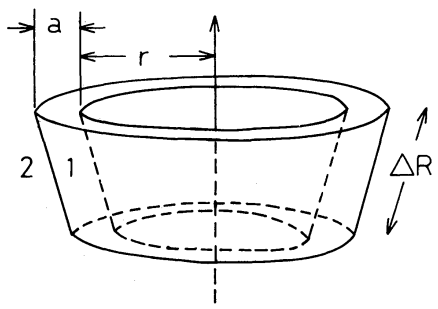


**Figure 3.** Slice of the surface layer to which momentum conservation is applied. Tangential stresses due to raidation act on the inner walls, while frictional forces due to turbulent mixing act on the outer walls.

(equation 11) representing momentum carried away by the outgoing radiation. We thus have a total radiative stress $\sigma$ given by

$$\sigma = \frac{3}{8c} F_{\mathrm{t,\,in}} - \frac{\gamma_1\beta_1 F_{\mathrm{s}1}}{c}$$

$$= \frac{3}{8c} F_{\mathrm{t,\,Sk}} - \frac{\gamma_1\beta_1(1+\gamma_1)(1-\beta_1)^2}{(1+\beta_1)^2}\frac{F_{\mathrm{s,\,Sk}}}{c}. \tag{16}$$

Here we have used (12), (13) and (7) to express $F_{\mathrm{t,\,in}}$ and $F_{\mathrm{s}1}$ in terms of $F_{\mathrm{t,\,Sk}}$ and $F_{\mathrm{s,\,Sk}}$. This tangential stress must be compared to the maximum value which can be carried in the turbulent shear flow, given by (6). If $\sigma < \sigma_{\max}$ we have the subsonic case and the velocity of layer 1 is given by (A12).

If $\sigma > \sigma_{\max}$ we have the supersonic case and layer 1 accelerates since it receives more momentum than layer 2 can drain away. The velocity of the second layer is now given by (A13). The condition for the supersonic case is $\sigma > \sigma_{\max}$, i.e.

$$0.375 F_{\mathrm{t}} - (1+\gamma_2)\gamma_2\beta_2 F_{\mathrm{s}1} > 0.367\,\alpha\gamma_2 F_{\mathrm{s}2}. \tag{17}$$

In this case, we can draw up the momentum balance for the surface element as follows. The rest mass entering the element (through the annular face) per unit time is given by $2\pi r a \rho_0 \gamma_1\beta_1 c$ and that leaving by the same expression evaluated at $R + \Delta R$. Clearly, a rest mass $\Delta m$ per unit time must be drawn into the surface layer from layer 2, where

$$\Delta m = \frac{d}{dR}(2\pi r a \rho_0 \gamma_1\beta_1 c)\Delta R.$$

This mass changes from velocity $\beta_2 c$ to $\beta_1 c$ and the associated change of momentum is given by $\Delta m(\gamma_1\beta_1 c - \gamma_2\beta_2 c)$. In addition, the mass entering the layer through the annular face gains speed, and the associated rate of change of momentum would be

$$\Delta P = 2\pi r a \rho_0 \gamma_1\beta_1 c \cdot \Delta R \cdot \frac{d}{dR}(\gamma_1\beta_1 c). \tag{18}$$

The total momentum change is equated to the net stress, which is given by (16) reduced by the drag term $\sigma_{\max}$ between layers 1 and 2. The consolidated momentum equation reads

$$\frac{d}{dR}\left(\frac{3\pi}{4\kappa}\gamma_1^2\beta_1^2 c^2 r\right) - \frac{d}{dR}\left(\frac{3\pi r}{4\kappa}\gamma_1\beta_1 c\right)\cdot\gamma_2\beta_2 c$$

$$= \frac{2\pi r}{c}\left\{0.375 F_{\mathrm{t,\,Sk}} - \gamma_1\beta_1\frac{(1+\gamma_1)(1-\beta_1)^2}{(1+\beta_1)^2}F_{\mathrm{s,\,Sk}} - 0.367\,\alpha\gamma_1(1+\beta_2\beta_{12})\right.$$

$$\left.\times\left(\frac{1-\beta_1}{1+\beta_1}\right)^2 F_{\mathrm{s,\,Sk}}\right\}. \tag{19}$$

Before studying the solution of this equation, we mention two implicit features. Usually, the radiative force is expressed in terms of an acceleration by the directed component and drag by the isotropic component. However, this can also be understood in terms of absorption followed by isotropic re-emission in the rest frame. The approach used above keeps track of momentum in the incoming and outgoing radiation and is thus physically equivalent to the usual treatment.

The second point concerns the radiative transfer of momentum across the 1–2 interface. The associated stress is $\simeq F_s\beta_{12}/c$. Since our drag term also has a similar structure, $\simeq 0.367\alpha(F_s/c)$, we note that this becomes important when

$$\beta_{12} \gtrsim 0.367\,\alpha. \tag{20}$$

In these cases, a higher effective value of $\alpha$ should operate. Apart from this complication, we consider this radiative momentum transfer to be absorbed in the turbulent drag, especially in view of the uncertainties regarding $\alpha$.

Only a brief description of how the equations of motion are solved is needed. Fig. 3 of Sk gives the necessary input values of the radiative fluxes $F_{s,\,Sk}$ and $F_{t,\,Sk}$ at various points along the funnel. We approximate the geometry by zones whose boundaries are given by straight line segments joining these points, and we approximate the variation of the fluxes by power laws in **r** over each such zone. At each point it is necessary to check whether we are in the subsonic or supersonic regime. In the first case, $\beta_1$ is given by (A12) with $v_*$ defined by (A3), and the stress $\sigma$ is given by (16). In the supersonic case we use the equation of motion (19) to compute $\beta_1$, while $\beta_2$ is given by (A13).

## 5 Results and discussion

The results of the calculations for three values of $\alpha$, viz., 0.3, 1 and 3, and for three values of $\beta_s$, viz., 0.01, 0.03 and 0.1, are given in Table 1. The particle luminosity $L_p$ at the top of the funnel (viz., at $r = 80\,GM/c^2$) is given in the funnel frame by

$$L_p = 4\pi r \cdot a\beta_1\rho_0 c\gamma_1(\gamma_1 - \gamma_{esc}), \tag{21}$$

where $\gamma_{esc}$ is the Lorentz factor corresponding to the escape velocity. When we recall that $a = 3/(8\kappa\rho_0)$ and divide by $L_E$ we find the dimensionless particle luminosity to be

$$l_p \equiv L_p/L_E = 0.375\,r\beta_1\gamma_1(\gamma_1 - \gamma_{esc}), \tag{22}$$

with **r** in units of $GM/c^2$. Table 1 gives our estimates of $l_p$ for the various cases studied. We notice that the largest value of the particle luminosity is about 1.5 times $L_E$. We now compare this to the results obtained by NN. They estimated a particle luminosity of $4L_E$

**Table 1.** Particle luminosity in units of the Eddington luminosity ($l_p$) calculated for various values of the sound speed ($\beta_s$) and the fraction coefficient ($\alpha$). The asterisks indicate those cases where radiative momentum transfer is important according to equation (20) and could alter the results. $c\beta_1$ and $c\beta_2$ are the velocities of the surface layer and the next layer respectively.

| $\beta_s$ | $\alpha$ | $\beta_1$ | $\beta_2$ | $l_p$ |
|---|---|---|---|---|
| | 0.3 | 0.38 | 0.03 | 1.0* |
| 0.01 | 1 | 0.23 | 0.06 | 0.2 |
| | 3 | 0.10 | 0.10 | 0.0 |
| | 0.3 | 0.39 | 0.05 | 1.1* |
| 0.03 | 1 | 0.30 | 0.11 | 0.4 |
| | 3 | 0.23 | 0.20 | 0.2 |
| | 0.3 | 0.43 | 0.02 | 1.5* |
| 0.1 | 1 | 0.40 | 0.05 | 1.2 |
| | 3 | 0.33 | 0.14 | 0.6 |

for the funnel model described in Sk. The outflow velocity they estimated corresponds to $\beta_1 = 0.4$ which is similar to the values in Table 1. However, their estimate of the penetration depth of the accelerating flux was $1/\kappa\rho$ rather than $3/8\kappa\rho$ and this accounts for the lower luminosity found here. That apart, the present work clarifies some aspects of the problem raised by NN. (a) The criterion used by NN for surface acceleration had the form $F_t \geqslant \alpha F_n$, and was based on an analogy with the Shakura–Sunyaev (1973) estimate of shear stresses in thin discs. Our criterion (17) still involves the ratio $F_t/F_s$, but now has as underlying physical mechanism (viz., turbulent mixing) and some velocity dependence. (b) The modification of the radiation field by the moving walls has been put in through equation (7) and this is an important effect. For a fixed total luminosity, we find that the radiation from moving walls carries away transverse momentum and also contributes to the transverse flux. Both these effects reduce the amount of tangential momentum actually available for accelerating the layer, as is clear from equation (16) for the stress. (c) The importance of mixing shear stresses described by $\alpha$ and the sound velocity $\beta_s$ becomes clear from Table 1. The maximum particle luminosity is obtained for low $\alpha$ and high $\beta_s$.

The asterisks in Table 1 indicate those cases where $\beta_{12} > 0.367\,\alpha$ at the top of the funnel (equation 20), showing that radiative momentum transfer across the 1–2 interface becomes important. However, the momentum transfer in the disc interior is still limited by $\alpha v_s^2/4.84$ from (5). Thus there will be acceleration of the second layer also in this case. While the sharing of momentum over a larger mass by itself tends to reduce the kinetic energy in the outflow, the reduced velocity can increase the accelerating stress (16), so it is not clear what the net effect on the particle luminosity will be.

One unsatisfactory aspect of the present work is that numerical results could be given for only one funnel model. However, this is a fairly typical model for a thick disc. Models with higher luminosities (e.g. Abramowicz *et al.* 1980) tend to need very large accretion rates and may not be of interest in the context of active galactic nuclei. On the low luminosity side, we have to fall back on the Newtonian estimates of particle luminosity made by NN (equation 19 of that paper) which should be applicable, since at low velocities, radiative drag effects are unimportant. We thus have

$$l_p = \frac{3}{16}\frac{r}{r_s}\left(\frac{Rr_s}{r^2}\right)^{3/2} l_r^{3/2} \tag{23}$$

where $l_r \equiv L_r/L_E$. Note that the penetration factor of 3/8 which was not used by NN is included in (23). From (23) we have $l_p = l_r$ when

$$l_r = \frac{256}{9}\left(\frac{r^4}{r_s R^3}\right).$$

In units with $G = M = c = 1$, typical values are $r \sim 100$, $R \sim 1000$, ($r_s = 2$) and we find that $l_p = l_r$ at $1.4\,L_E$. However, from the results of this paper, the various drag effects are already significant at this stage. So equation (23) is applicable only at somewhat lower luminosities.

It is interesting to compare the momentum carried in the particle beam with the estimate given in Section 1. At a point near the bottom of the funnel where $r = 16$, the self-flux $F_s$ in Sikora's model is given by $F_s\kappa = 0.09$, and the associated rate of momentum transfer at this cross-section is $(4\pi/3)r^2F_s = 96/\kappa$. The momentum escaping in a beam of $(8.5/2)L_E$ (for one funnel) equals $53/\kappa$ (since $L_E = 4\pi/\kappa$). The maximum momentum which the particle beam can carry is thus $43/\kappa$, i.e. somewhat less than that contained in the radiation. For $\beta_1 = 0.4$, this corresponds to an energy outflow of $1.4\,L_E$ (from both funnels). This is in reasonable agreement with the particle luminosity we compute in the $\alpha = 0.3$ case and with calculations for smaller $\alpha$, not shown in Table 1, providing a consistency check on the

assumptions made concerning the radiation field and accelerating forces. Of course, when the turbulent mixing is efficient, i.e. for higher values of $\alpha$, the excess momentum is taken up by the disc and only a small fraction emerges in the particle beam.

There are two further effects which tend to enhance the particle luminosity. If the outflowing matter makes the funnel optically thick, the coupling between the matter and radiation will be more efficient. Further, the energy dissipated by turbulent mixing will act to raise the local sound velocity and thus favour larger values of $L_p$. However, large values of $\gamma$ seem unlikely, at least for optically thin funnels. It appears that the main role of the mass outflow in this case is to modify the radiation field in the funnel, and, to a lesser extent, carry away a portion of the luminosity. Further self-consistent calculations of these effects would be of interest.

## Acknowledgments

We thank our referee, D. B. Wilson, for his detailed and constructive comments on an earlier version of the paper. PJW thanks the Raman Research Institute for hospitality and gratefully acknowledges support from a Smithsonian Institution foreign currency research travel grant, and from NSF grant AST 82-11065.

## References

Abramowicz, M. A. & Piran, T., 1980. *Astrophys. J.*, **241**, L7.
Abramowicz, M. A., Calvani, M. & Nobili, L., 1980. *Astrophys. J.*, **242**, 772.
Abramowicz, M. A., Calvani, M. & Nobili, L., 1983. In preparation.
Blandford, R. D. & Pringle, J. E., 1977. *Mon. Not. R. astr. Soc.*, **176**, 443.
Elmegreen, B., 1979. *Astr. Astrophys.*, **80**, 77.
Jaroszyński, M., Abramowicz, M. A. & Paczyński, B., 1980. *Acta. Astr.*, **30**, 1.
Kozlowski, M., Jaroszyński, M. & Abramowicz, M. A., 1978. *Astr. Astrophys.*, **63**, 209.
Landau, L. D. & Lifshitz, E. M., 1959. *Fluid Mechanics*, Pergamon Press, Oxford.
Lynden-Bell, D., 1978. *Phys. Scripta*, **17**, 185.
Meier, D., 1982a. *Astrophys. J.*, **256**, 681.
Meier, D., 1982b. *Astrophys. J.*, **256**, 693.
Meier, D., 1982c. *Astrophys. J.*, **256**, 706.
Monin, A. S. & Yaglom, A. M., 1971. *Statistical Fluid Mechanics*, MIT Press.
Nityananda, R. & Narayan, R., 1982. *Mon. Not. R. astr. Soc.*, **201**, 697 (NN).
Paczyński, B. & Wiita, P. J., 1980. *Astr. Astrophys.*, **88**, 23.
Piran, T., 1982. *Astrophys. J.*, **257**, L23.
Rees, M. J., Begelman, M. C., Blandford, R. D. & Phinney, E. S., 1982. *Nature*, **295**, 17.
Shakura, N. I. & Sunyaev, R. A., 1973. *Astr. Astrophys.*, **24**, 337.
Sikora, M., 1981. *Mon. Not. R. astr. Soc.*, **196**, 257 (Sk).
Sikora, M. & Wilson, D. B., 1981. *Mon. Not. R. astr. Soc.*, **197**, 529 (SW).
Turland, B. D. & Scheuer, P. A. G., 1977. *Mon. Not. R. astr. Soc.*, **176**, 421.
Wiita, P. J., 1982. *Astrophys. J.*, **256**, 666.

## Appendix A: Mean velocity and shear in the mixed region

We first consider an auxiliary problem, viz., a cylinder with a tangential stress $\sigma$ parallel to its axis (which we take along $R$) acting on its walls and being transmitted by turbulent mixing through a fluid of density $\rho$ occupying the space $Y_1 > r$. Here $r$ is the radius of the cylinder and $Y_1$ the distance from the axis. We write $Y = Y_1 - r$. Let $U(Y)$ be the steady state velocity parallel to the axis set up in the fluid. According to the mixing length theory (Monin & Yaglom 1971) the shear stress is given by $\rho l_m^2 (\partial U/\partial Y)^2$. As is usual, we take the mixing length $l_m$ to be equal to $AY$, where the constant $A^{-1}$ is approximately 2.4 in the

related problem of flow past a wall (Landau & Lifshitz 1959). Conservation of the $R$ component of momentum then gives

$$2\pi r\sigma = 2\pi(r+Y)A^2Y^2\rho\left(\frac{\partial U}{\partial Y}\right)^2. \tag{A1}$$

This leads to the solution (satisfying $U \to 0$ as $Y \to \infty$)

$$U = 2.4\,v_* \ln\left(\frac{\sqrt{1+Y/\pi}+1}{\sqrt{1+Y/r}-1}\right) \tag{A2}$$

$$\simeq 2.4\,v_* \ln(4r/Y) \qquad (\text{for } Y \lesssim r) \tag{A3}$$

where

$$v_*^2 = \sigma/\rho. \tag{A4}$$

However, this velocity field is not directly applicable to our problem because of the steady state assumption, which effectively neglects inertial terms, i.e. the acceleration of the fluid in the $R$-direction. The momentum current associated with the flow (A3) is given by

$$P \simeq \int_0^{4r} 2\pi(r+Y)\rho U^2(Y)\,dY \simeq 2\pi r^2\rho v_*^2 \cdot 16 \times (2.4)^2 \cdot 3/4. \tag{A5}$$

We can define a length scale $R_{\text{eff}}$ such that

$$2\pi r R_{\text{eff}}\sigma = P. \tag{A6}$$

The injected momentum over a length $R_{\text{eff}}$ of the wall equals that carried in the flow. From (A5) and (A6) we find

$$R_{\text{eff}} \simeq 12 \times (2.4)^2 r. \tag{A7}$$

It is clear from (A7) that the steady-state situation is attained only over length scales of the order of $10^2 r$. Since the funnel under discussion is not in this regime we incorporate inertial effects in a heuristic manner as follows. Consider a velocity field

$$U(Y) = 2.4\,v_* \ln\left[\frac{4\,d(R)}{Y}\right]. \tag{A8}$$

(A8) is just (A2) modified to allow a depth of penetration, $d(R)$, which varies with distance $R$ along the funnel. Just as in (A5), we can calculate the momentum current associated with this velocity field. We find

$$P(d) \simeq 16\pi r d\ (2.4)^2 \rho v_*^2 \tag{A9}$$

where we have taken $d < r$ as justified by the result and neglected $d^2$ compared to $rd$. Equating $P(d)$ to the total momentum injected up to the point $R$, viz., $2\pi r\sigma$, we find $d(R) \simeq R/46$. With this choice of $d$ we have the velocity field

$$U(R, Y) = 2.4\,v_* \ln(R/11.5\,Y). \tag{A10}$$

Although (A10) does not satisfy the detailed momentum balance in each element $dRd$, it satisfies the global condition (A6) and this is sufficient for our purpose. The treatment of the flow in the mixed region has been non-relativistic. While we do not have a fully relativi-

stic treatment, it seems reasonable to incorporate relativistic velocity addition by rewriting (A10) as follows

$$U(R, Y) = c \tanh\left[\frac{2.4 v_*}{c} \ln\left(\frac{R}{11.5\, Y}\right)\right]. \tag{A11}$$

In the subsonic case, as explained in the main text, the mixing is able to transfer all the injected momentum into the interior. The velocity $v_1$ of the first layer is then given by

$$\beta_1 = \frac{U(R, a)}{c} = \tanh\left[2.4 \frac{v_*}{c} \ln\left(\frac{R}{11.5a}\right)\right]. \tag{A12}$$

In the supersonic case, we have $v_*^2 = \alpha v_s^2/4.84$ (equation 5). The velocity of the second layer is then given by

$$\beta_2 = \tanh\left[\frac{2.4\, \alpha^{1/2} v_s}{2.2\, c} \ln\left(\frac{R}{11.5a}\right)\right]. \tag{A13}$$

The layer thickness, $a = 3/8\, \kappa \rho_0$ can be calculated through equation (14)

$$a = 27 c^3 \beta_s^2/(128\, \kappa F_{s2}). \tag{A14}$$

The stress due to mixing in the supersonic case has its maximum value $\sigma_{max} = \alpha \rho v_s^2/4.84$. Associated with this stress is also an energy current since the 1 layer is losing energy to the drag forces. Both these quantities are in the frame of layer 2. Returning to the funnel frame, we have

$$\sigma_{max} = \frac{\alpha \rho v_s^2}{4.84} \gamma_2 (1 + \beta_2 \beta_{12}). \tag{A15}$$

This is equation (6) of the main text.

## Appendix B

The incoming radiation field at any point on the funnel surface is very intense for rays coming from the interior ($n_R$ tending to +1 in the notation of Section 3.2) and vanishes for rays coming from the opening ($n_R = -1$). A simple analytic form with these properties is

$$I(\mathbf{n}) = I_0 \frac{1 + n_R}{1 - \lambda n_R} \tag{B1}$$

where the parameter $\lambda$ can range from $-1$, describing an isotropic radiation field, to $+1$, which gives a field peaking sharply for rays coming from the interior of the funnel. $F_t$, $F_n$ and $T^{RY}$ can be calculated for this field (B1) and the results are given below

$$F_t/\pi I_0 = \frac{(1+\lambda)}{\lambda^2}\left[\frac{1}{\lambda} \ln\left(\frac{1+\lambda}{1-\lambda}\right) - 2\right] \tag{B2}$$

$$F_n/\pi I_0 = \left[2 + \frac{\lambda}{1 + (1-\lambda^2)^{1/2}}\right] \Big/ \left[1 + (1-\lambda^2)^{1/2}\right] \tag{B3}$$

$$c T^{RY}/\pi I_0 = \frac{1}{(1-\lambda)}\left\{\frac{1}{[1 + (1-\lambda^2)^{1/2}]} - \frac{(3+\lambda^2)}{4[1 + \lambda^2/2 + (1-\lambda^2)^{-1/2}]}\right\}. \tag{B4}$$

**Table 2.** The parameter λ, defined by equation (B1), measures the anisotropy of the incoming radiation at a point on the funnel surface. The next row gives the ratio of tangential to normal fluxes, and the third row the optical depth of the layer feeling the accelerating force.

| λ | −0.8 | −0.1 | 0.9 |
|---|---|---|---|
| $F_t/F_n$ | 0.498 | 1.235 | 3.261 |
| $cT^{RY}/F_t$ | 0.335 | 0.375 | 0.307 |

Table 2 shows the behaviour of $F_t/F_n$ and $cT^{RY}/F_t$ for three values of λ.

Even for a rather anisotropic field, corresponding to $F_t/F_n = 3.26$, we find that the penetration optical depth is greater than 0.3, not too far from the value of 0.375 for dipole anisotropy which we have adopted for simplicity in the main text (equation 10). For comparison, the range of $F_t/F_n$ in the region of interest for Sikora's model funnel is about 0.5–2.5.